IEICE TRANS. COMMUN., VOL.E85–B, NO.4 APRIL 2002

PAPER

Reverse Link Bandwidth Efficiency of a Spectrally Overlapped CDMA System

Duk Kyung KIM[†], *Nonmember and* **Fumiyuki ADACHI**[††], *Member*

SUMMARY The reverse link bandwidth efficiency of a spectrally overlapped CDMA system with fast transmit power control is evaluated to find the optimum overlapping, where the bandwidth efficiency is defined as the maximum aggregate bit rate of all subsystems per unit bandwidth (bps/Hz). Single and multiple cell environments are considered. Besides the rectangular chip pulse, the impact of a pulse-shaping filter is discussed. It is found that the raised cosine spectrum pulse shaping helps to increase the bandwidth efficiency and strict pulse shaping filter problem can be avoided if a large number of subsystems are overlapped. It is also found that the optimum carrier spacing remains unchanged irrespective of the power delay profile shape of the multipath channel, whether multipath fading exists or not, and whether a single cell or multiple cell system is considered. However, the bandwidth efficiency strongly depends on them and the impacts of the related parameters are discussed.

key words: *Spectrally overlapped CDMA system, pulse shaping filter, fast power control, multiple cell, multipath fading*

1. Introduction

After successful launch of the second generation mobile communications systems such as GSM, PDC, and IS-95, the number of subscribers has been dramatically increasing [1]. Furthermore, in 2001 a new-generation system called International Mobile Telecommunications (IMT)-2000 is expected to start service and extend service capabilities from voice and low rate data to multimedia and high rate data [2]. However, unfortunately, the frequency bandwidth allocated to each operator is limited and therefore, it is quite important how to efficiently use the given bandwidth, i.e., how to maximize the supportable number of users (*or* the aggregate data rate) with a given bandwidth.

One of attractive features of direct sequence code division multiple access (DS-CDMA or shortly CDMA), which is strongly considered for IMT-2000 systems [3], is the coexistence with other CDMA systems operating in the same frequency band [4], [5]. Observing the spectrum of CDMA signal, we can find that the power is mainly concentrated around the center of the band. And therefore, overlapping the spreading bands of neighboring subsystems is expected to yield a certain amount of increase in bandwidth efficiency. One of its realization is overlaid multiband CDMA systems [5], where 5/10/20 MHz bands are overlapped to flexibly accommodate a variety of services, additionally yielding a small gain in bandwidth efficiency [6]. Another way is to partially overlap a number of narrowband CDMA subsystems. Shilling and Pickholtz [7] first suggested such overlapped systems. Han and Kim [8], [9] found out that the optimal amount of overlapping is half null-to-null (i.e., main robe) bandwidth for a rectangular chip pulse shaping and that the optimum number of overlapped subsystems exists in a multipath fading environment. They also compared its performance with that of a single wideband CDMA system to show that whether a spectrally overlapped system can yield better performance or not depends on the bit error rate requirement and propagation channel model. However, these works didn't take into account the chip pulse shaping filter and fast transmit power control (TPC), and furthermore focused on a single cell environment. Therefore, the impacts of the chip pulse shaping filter, the fast TPC, and other cell interference are still in question. All of these questions are answered in this paper.

In this paper, we introduce the bandwidth efficiency defined as the maximum aggregate bit rate of all subsystems per unit bandwidth (bps/Hz) and evaluate the reverse link bandwidth efficiency of a spectrally overlapped CDMA system with signal-to-interference ratio (SIR)-based fast TPC in multiple cell and multipath fading environments. For computing the interference power assuming arbitrary chip pulse shape, arbitrary spreading bandwidth, and arbitrary frequency overlapping, Adachi and Kim's computing method [10] is applied. For analyzing the bandwidth efficiency of a multiple cell system with SIR-based fast TPC, we apply Kim and Sung's methodology proposed for the reverse link capacity estimation [11], [12]. In this paper, then, we discuss the effect of the pulse shaping filter and how much gain in the bandwidth efficiency can be obtained by spectral overlapping. Also discussed are the impacts of the number of overlapped subsystems, the TPC target of signal energy per information bit-to-interference plus background noise power spectrum density ratio E_b/I_o, and propagation parameters (path

Manuscript received April 3, 2001.
Manuscript revised October 10, 2001.

[†]The author was with the Wireless Lab., NTT DoCoMo, Inc., Japan and is presently with the School of Information & Communication Engineering, Inha university, Inchon, 402-751 Korea.

[††]The author was with the Wireless Lab., NTT DoCoMo, Inc., Japan and is with the Department of Electrical Communications at Graduate School of Engineering, Tohoku University, Sendai, 980-8579 Japan.

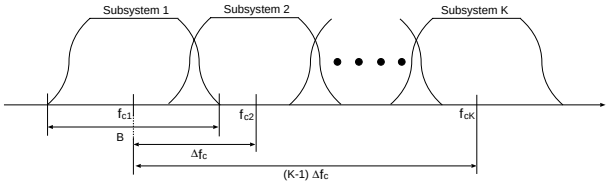

Fig. 1 System model: An example case.

loss exponent and shadowing standard deviation), and the number of Rake fingers.

This paper is organized as follows. Section 2 describes the system considered and investigates the impact of pulse shaping filter on interference suppression factor, wherein raised cosine spectrum pulse shaping is considered. Section 3 examines a non-fading channel as a first step for evaluation, which provides easy understanding as well as the performance upper bound for a multipath fading channel. Then, Sect. 4 extends the analysis to multipath Rayleigh fading channels with uniform and exponential power delay profiles and examines the impact of multipath fading. Section 5 compares the bandwidth efficiencies for both non-fading and multipath fading environments and investigates the effects of various parameters such as the roll-off factor of raised cosine spectrum pulse shaping filter, the number of overlapped subsystems, the target E_b/I_o, the propagation parameters, and the number of Rake fingers. Finally, we draw our conclusions in Sect. 6.

2. System Description

2.1 Cell Configuration

The followings are assumed for cell configuration:

- Ideal hexagonal cell structure with a unit cell radius.
- The zero-th cell and 18 other cells indexed t in the first and second tiers.
- Users are uniformly distributed in space.
- The path loss exponent of μ and the log-normal shadowing with standard deviation σ dB and mean = 0 dB.
- The best cell site that has the least product of path loss and shadowing is always selected to communicate with (this is equivalent to selection type of soft handoff).

2.2 Spectrally Overlapped System

Figure 1 illustrates an example case of overlapped CDMA system, where only two neighboring subsystems are overlapped and the total number of subsystems is K. All subsystems are assumed to have identical chip rate $1/T_c$ and identical pulse shaping, i.e., the spreading bandwidth B of each subsystem is the same. In this paper, all subsystems are equally spaced in carrier frequency and the carrier spacing is denoted by Δf_c. If Δf_c is less than the spreading bandwidth B, the neighboring subsystems are overlapped. The total spreading bandwidth W can be given by

$$\begin{aligned} W &= \frac{B}{2} + (K-1)\Delta f_c + \frac{B}{2} \\ &= B + (K-1)\Delta f_c. \end{aligned} \tag{1}$$

2.3 Impact of Pulse Shaping Filter

The spectrum of CDMA signal depends on the chip pulse shaping filter and hence, it is clear that the performance of a overlapped system varies according to the characteristic of the chip pulse shaping filter. In CDMA systems, the interference power after receiver matched filtering is reduced to $\frac{\xi}{F}P$ for random spreading code, where P is the received interference power at the receiver input, F is the spreading factor, and $\xi(\leq 1)$ is the interference suppression factor. The interference suppression factor depends on the characteristic of pulse shaping filter and can be computed using [10] (how to compute the interference suppression factor is summarized in Appendix A). In this paper, the overall filter response is assumed to satisfy the Nyquist condition so that the inter-symbol interference (ISI)-free condition is kept. The transmit and receive filters are assumed to be the square root of Nyquist filter.

The raised cosine spectrum shape is widely used in practice and the composite transfer function $H(f)$ of transmitter and receiver filters is given by [13]

$$H(f) = \begin{cases} 1 & , \text{ for } 0 \leq |f-f_c| < \frac{1-\alpha}{2T_c}, \\ \frac{1}{2}\left[1-\sin\left(\frac{2\pi|f-f_c|T_c-\pi}{2\alpha}\right)\right] & , \text{ for } \frac{1-\alpha}{2T_c} \leq |f-f_c| \leq \frac{1+\alpha}{2T_c}, \\ 0 & , \text{ otherwise,} \end{cases} \tag{2}$$

where α $(0 \leq \alpha \leq 1)$ is the roll-off factor and f_c is the carrier center frequency. The pass band and accordingly, spreading bandwidth B becomes $(1+\alpha)/T_c$. On the other hand, for the case of rectangular chip pulse as assumed in [8], [9], Eq. (2) can be rewritten as

$$H(f) = \left[\frac{\sin(\pi(f-f_c)T_c)}{\pi(f-f_c)T_c}\right]^2, \tag{3}$$

for which, the spreading bandwidth B is defined as the main robe bandwidth and set $B = 2/T_c$.

The interference suppression factor ξ_{ii} from a user to another user both in the same subsystem is given by from Appendix A and also [14]

$$\xi_{ii} = \begin{cases} 1-\frac{\alpha}{4} & , \text{ for a raised cosine spectrum pulse,} \\ 2/3 & , \text{ for a rectangular pulse.} \end{cases}$$

Figure 2 shows the interference suppression factor ξ_{21} for a raised cosine spectrum pulse shaping filter and

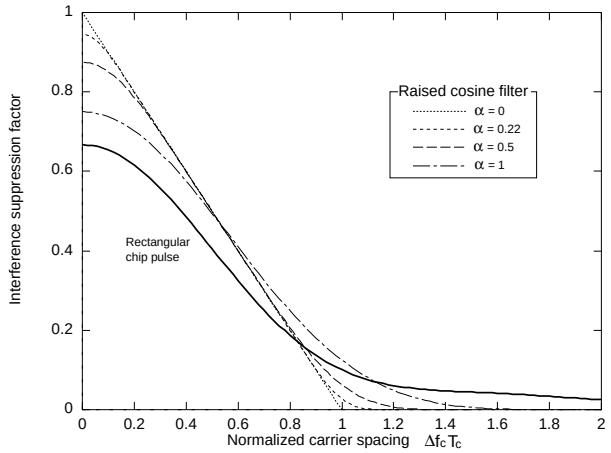

Fig. 2 Interference suppression factors ξ_{21} versus the normalized carrier spacing $\Delta f_c T_c$ for a raised cosine spectrum pulse shaping filter and a rectangular pulse.

a rectangular chip pulse as a function of the normalized carrier spacing $\Delta f_c T_c$. This result can be directly used for any two subsystems i and j. For $\alpha = 0$, the interference suppression factor linearly decreases as $\Delta f_c T_c$ increases (this can be easily understood from the fact that the filter frequency response becomes rectangular shape in this case). However, nonlinear decrease can be observed for other values of α, especially around the region where $\Delta f_c T_c \leq 0.2$ or $\Delta f_c T_c \geq 0.8$, due to slow decay of filter frequency response near bandwidth boundaries (see the shape of filter frequency response in Fig. 1). In the case of rectangular chip pulse, it is interesting to note that the interference suppression factor is non-zero even when $\Delta f_c T_c$ approaches 2 because this pulse is time-limited.

3. Reverse Link Bandwidth Efficiency in a Non-fading Environment

Let's first consider a non-fading environment. A single type of constant bit rate (CBR) traffic is considered for K overlapped subsystems, where the information bit rate is the same for all users and is denoted as R_b (bps) and all subsystems have the same processing gain of G (defined as the chip rate/information bit rate $= (R_b T_c)^{-1}$). Let's consider N_k users are in communication in a subsystem k and their received signal power at the home BS is denoted as S_k, which is a random variable according to the interference level in SIR-based fast TPC systems.

3.1 E_b/I_o Equation

E_b/I_o of users in a subsystem m can be expressed as

$$\left(\frac{E_b}{I_o}\right)_m \triangleq \frac{GS_m}{\sum_{k=1}^{K} \xi_{km} N_k S_k - \xi_{mm} S_m + I_m + 1} \quad (4)$$

where I_m is the other cell interference power contributed from all subsystems $k = 1 \sim K$ to a subsystem m. ξ_{km} is the interference suppression factor from a subsystem k to a subsystem m and is derived in Appendix A. It is noted that, in Eq. (4), signal power and interference power are normalized by the background noise power η_o/T_c (the equivalent noise bandwidth is the same for both raised cosine Nyquist spectrum chip pulse shaping filter and the rectangular chip pulse and is given by $1/T_c$), where $\eta_o/2$ is the two-sided background noise power spectrum density (thus, now S_m and I_m denote the signal-to-noise power ratio (SNR) and the interference-to-noise power ratio (INR), respectively). The definition in Eq. (4) is based on a Gaussian density approximation to evaluate the bit error rate (BER) in an asynchronous DS-CDMA system when an additive white Gaussian noise (AWGN) process and a random signature sequences are assumed.

3.2 Statistics of the Signal Power with SIR-based Fast TPC

The link is assumed to enter an outage state if the required signal power level is greater than the maximum allowable value $S_{\max}$ or mathematically if it is below zero (when too many users are accommodated in a system, the required signal power level can be calculated as a negative value [11], [12]). We need to know $E[S_m]$ and $E[S_m^2]$ to compute the outage probability. How to obtain them is described below.

A Gaussian model is adopted for other cell interference power I_m in a subsystem m. From Eqs. (A· 2) and (A· 3) in Appendix B, the mean m_{I_m} and variance $\sigma_{I_m}^2$ of I_m can be expressed using $E[S_m]$ and $E[S_m^2]$ as:

$$m_{I_m} = M(\mu,\sigma) \sum_{k=1}^{K} \xi_{km} N_k E[S_k], \quad (5)$$

$$\sigma_{I_m}^2 = \sum_{k=1}^{K} \xi_{km}^2 N_k \left(A(\mu,\sigma) E[S_k^2] - B(\mu,\sigma) E^2[S_k] \right), \quad (6)$$

where $E[\cdot]$ denotes the ensemble average. The above equations are used to compute $E[S_m]$ and $E[S_m^2]$.

Assuming all users are power controlled to maintain minimum power levels satisfying $(E_b/I_o)_m = \gamma$, Eq. (4) can be rewritten as

$$\sum_{k=1}^{K} \xi_{km} N_k S_k + I_m + 1 = \left(\xi_{mm} + \frac{G}{\gamma}\right) S_m, \text{ for all } m. \quad (7)$$

By taking the expectation of both sides of Eq. (7) and by substituting Eq. (5) into Eq. (7), the following relations are obtained

$$(1+M(\mu,\sigma))\sum_{k=1}^{K}\xi_{km}N_kE[S_k]+1=\left(\xi_{mm}+\frac{G}{\gamma}\right)E[S_m],\ \text{for all } m. \tag{8}$$

By solving Eq. (8), $E[S_m]$ is obtained.

To compute $E[S_m^2]$, we first express Eq. (7) as

$$\mathbf{AS}=\mathbf{B}, \tag{9}$$

where

$$\mathbf{S}=\begin{bmatrix} S_1 \\ \vdots \\ S_K \end{bmatrix},$$

$\mathbf{A}$ is a $K\times K$ matrix, and $\mathbf{B}$ is a $K\times 1$ column vector. The elements a_{mk} of $\mathbf{A}$ can be given by

$$a_{mk}=\begin{cases} \xi_{mm}+\frac{G}{\gamma}-\xi_{mm}N_m & ,\ \text{if } m=k \\ -\xi_{km}N_k & ,\ \text{otherwise} \end{cases} \tag{10}$$

and the elements b_k of $\mathbf{B}$ can be expressed as

$$b_k=I_k+1. \tag{11}$$

From Eq. (9), $\mathbf{S}$ can be obtained by

$$\mathbf{S}=\mathbf{A}^{-1}\mathbf{B}\triangleq\mathbf{CB}. \tag{12}$$

Therefore, S_m can be expressed as the weighted sum of INR in each subsystem. If the other cell interference in each subsystem is assumed to be mutually independent one another, the variance of S_m can be obtained as the sum of the variances of other cell interference. Hence $E[S_m^2]$ can be easily obtained from Eq. (12):

$$E[S_m^2]=\sum_{k=1}^{K}c_{mk}^2\sigma_{I_k}^2+E^2[S_m], \tag{13}$$

where c_{mk} is an element in the m-th row and k-th column of $\mathbf{C}$.

After obtaining $E[S_m]$ for all m from Eq. (8), the steps for calculation of $E[S_m^2]$ are as follows:

1. Set all $\sigma_{I_m}^2$ at zeros.
2. Calculate $E[S_m^2]$ from Eq. (13).
3. Calculate $\sigma_{I_m}^2$ from Eq. (6).
4. Repeat steps 2 and 3 until the difference between old and new values of $E[S_m^2]$ is within a given bound. For numerical examples, the difference is set to be less than 1 %.

3.3 Computing the Bandwidth Efficiency

From the mean and variance statistics of S_m for all m from Eqs. (8) and (13), the outage probability can be obtained for each subsystem [11]. If $P_{k,out}$ is the outage probability of a subsystem k and $\mathbf{N}$ is the matrix of N_k $(1\le k\le K)$, the admissible region can be expressed as $\mathbf{N}$ satisfying

$$P_{k,out}\le o,\ \text{for all } k, \tag{14}$$

where o is the maximum allowable outage probability and is assumed to be the same for all k for simplicity. Now, let the link capacity be $N_{\max}$ which is the sum of $N_{k,\max}$ for all k. We introduce the bandwidth efficiency as a performance measure:

$$\eta\triangleq\frac{R_b\sum_{k=1}^{K}N_{k,\max}}{W}\triangleq\frac{N_{\max}/G}{WT_c}(bps/Hz), \tag{15}$$

where R_b is the information bit rate of each user.

4. Multipath Fading Environment

Now let's consider a multipath fading environment. First, multipath Rayleigh fading channel is characterized by two power delay profiles: Uniform and exponential power delay profiles. Then, instantaneous received signal power is derived under ideal fast TPC with a Rake receiver with R finger based on maximal ratio combining. The sum of interference from other users is well approximated as a Gaussian noise, when observed over a short-term time interval (which is defined as a time interval necessary to remove the instantaneous channel variations due to fading but not to remove those due to shadowing), due to central limit theorem for a large number of users. So we use this approximation [16]–[18] and thus, the transmission quality represented by BER can be evaluated using the signal energy per information bit-to-*short term average* interference plus background noise power spectrum density ratio E_b/I_o.

4.1 Channel Model

A DS-CDMA receiver can resolve the multipath channel into several frequency nonselective paths with discrete time delays of a multiple of chip duration T_c. It is assumed in this paper that each resolvable propagation path endures the same attenuation according to the distance and the same shadowing. The equivalent lowpass impulse response of the multipath fading channel between the user of interest and the BS can be expressed as [18], [19]

$$h(t,\tau)=\sum_{l=0}^{\infty}\xi_l(t)\delta(\tau-\tau_l), \tag{16}$$

where $\xi_l(t)$ and τ_l are the complex-valued path gain and time delay of the l-th path, respectively, and $\delta(x)$ is the delta function. Since the fading maximum Doppler frequency can in most practical cases be assumed to be very low compared to the data modulation symbol rate [19], the time dependency of the path gain is dropped hereafter. If a_l denotes $|\xi_l|^2$, a_l satisfies the following

condition:

$$\sum_{l=0}^{\infty} E[a_l] = 1. \tag{17}$$

Assuming a wide sense stationary uncorrelated scattering (WSSUS) channel model, a_l is exponentially distributed [13].

The multipath fading channel can be characterized by its power delay profile. Two power delay profile shapes are assumed in this paper: Uniform power delay profile and exponential power delay profile.

$$E[a_l] = \begin{cases} \frac{1}{L}, 0 \le l \le L-1 \\ \quad \text{, for a uniform profile} \\ (1-e^{-\epsilon})e^{-\epsilon l}, l \ge 0 \\ \quad \text{, for an exponential profile,} \end{cases} \tag{18}$$

where L is the total number of paths in a uniform power delay profile. In an exponential power delay profile, L is implicitly set at infinity and ϵ is a decay factor. If 90 % of signal power can be captured on average by using from zero-th path to the $L_{90\%}$-th path, $L_{90\%}$ is equal to $2.3/\epsilon$.

4.2 Instantaneous Received Signal Power

Let $a_{m,l}^{(n)}$ denote the squared path gain of the l-th path from n-th user in a subsystem m. $a_{m,l}^{(n)}$'s are exponentially distributed and mutually independent for different m, l, and n, whose means are determined only by the path index l. The multipath fading experienced after Rake combining with R fingers of n-th user in a subsystem m can be represented by

$$X_m^{(n)} \triangleq a_{m,0}^{(n)} + \ldots + a_{m,R-1}^{(n)}. \tag{19}$$

Assuming ideal fast TPC, the transmit power is controlled so that the instantaneous received signal power becomes the minimum power level S_m satisfying the received E_b/I_o = the target value. Hence, the instantaneous signal power $\widetilde{P}_m^{(n)}$ received at antenna can be expressed as [20]

$$\widetilde{P}_m^{(n)} = S_m \left[1 + \frac{a_{m,R}^{(n)} + \ldots}{X_m^{(n)}} \right]. \tag{20}$$

On the other hand, $\widetilde{P}_m^{(n)}$ is just S_m in a non-fading environment.

4.3 Computing the Bandwidth Efficiency

Since assuming an ideal Rake combiner with R finger, the E_b/I_o of the zero-th user of the zero-th cell in a subsystem m is the sum of the E_b/I_o of each path and can be expressed as [18], [19]:

$$\left(\frac{E_b}{I_o}\right)_m = \sum_{r=0}^{R-1} \left(\frac{E_b}{I_o}\right)_{m,r}, \tag{21}$$

where $\left(\frac{E_b}{I_o}\right)_{m,r}$ is the E_b/I_o of r-th path in a subsystem m and, from Eq. (20), is given by Eq. (22) at the top of the next page, where I_m is the other cell interference power contributed from all subsystems $k = 1 \sim K$ to a subsystem m. The statistical expectation in denominator is introduced to obtain short term average of the interference from other users in the same cell. In Eq. (22), we have assumed that all users' received signals are time asynchronous because of the reverse link and that the time delay τ_l of the l-th path varies and thus, all paths are considered time asynchronous. R paths are selected to have the highest power on average.

For a large number of users, $a_{m,r}^{(0)}$ in the denominator has a negligible impact and can be omitted. Since $a_{k,l}^{(n)}$ for $l > M$ and $X_k^{(n)}$ are mutually independent, substitution of Eq. (22) into Eq. (21) yields

$$\left(\frac{E_b}{I_o}\right)_m \approx \frac{GS_m}{\sum_{k=1}^{K} \xi_{km} S_k N_k (1+D) + I_m + 1}, \tag{23}$$

where D can be expressed as

$$D = \sum_{l=R}^{\infty} E\left[\frac{a_{k,l}^{(n)}}{X_k^{(n)}}\right] \triangleq E[\frac{1}{X}] D_a \tag{24}$$

and D_a is given by

$$\begin{aligned} D_a &\triangleq \sum_{l=R}^{\infty} E\left[a_{k,l}^{(n)}\right] \\ &= \begin{cases} (L-R)\frac{1}{L}, & \text{for the uniform profile} \\ e^{-\epsilon R}, & \text{for the exponential profile.} \end{cases} \end{aligned} \tag{25}$$

Assuming all users are power controlled to maintain minimum power levels satisfying $(E_b/I_o)_m = \gamma$, Eq. (23) can be rewritten as

$$\begin{aligned} \sum_{k=1}^{K} \xi_{km} S_k N_k (1+D) + I_m + 1 \\ = \frac{G}{\gamma} S_m, \text{ for all } m. \end{aligned} \tag{26}$$

From Eqs. (A·5) and (A·6), the mean m_{I_m} and variance $\sigma_{I_m}^2$ of I_m can be expressed as:

$$m_{I_m} = M(\mu,\sigma) E[\frac{1}{X}] \sum_{k=1}^{K} \xi_{km} N_k E[S_k], \tag{27}$$

$$\begin{aligned} \sigma_{I_m}^2 = E^2[\frac{1}{X}] \sum_{k=1}^{K} \xi_{km}^2 N_k \big(A(\mu,\sigma) E[S_k^2] \\ - B(\mu,\sigma) E^2[S_k] \big). \end{aligned} \tag{28}$$

The remaining procedures to obtain $E[S_m]$ and $E[S_m^2]$ are the same as in Sect. 3.

As a special case, in a single cell system, Eq. (26) is simplified as

$$\left(\frac{E_b}{I_o}\right)_{m,r} \triangleq \frac{GS_m \frac{a_{m,r}^{(0)}}{X_m^{(0)}}}{\sum_{k=1}^{K} \xi_{km} S_k E \left[\sum_{n_k=0}^{N_k-1} \sum_{l=0}^{\infty} \frac{a_{k,l}^{(n_k)}}{X_k^{(n_k)}} - \frac{a_{m,r}^{(0)}}{X_m^{(0)}}\right] + I_m + 1}, \quad (22)$$

Table 1 System parameters

G	128
$1/T_c$	4.096 Mcps
γ	3.34 dB
$S_{\max}$	0 dB
α (roll-off factor)	0.22
K	4
o	0.01
μ	4
σ	8 dB

$$\sum_{k=1}^{K} \xi_{km} S_k N_k (D+1) + 1 = \frac{G}{\gamma} S_m, \text{ for all } m. \quad (29)$$

Since $\xi_{mm} \leq 1$ and $\frac{G}{\gamma} \gg \xi_{mm}$, the bandwidth efficiency in this case is just scaled down by a factor of $1/(1+D)$ compared to a non-fading case in Eq. (7). Furthermore, if $R = L$ in a uniform power delay profile, $D = 0$ and hence, the bandwidth efficiency is the same as in a non-fading environment.

5. Numerical Examples

Table 1 shows the system parameters, which will be assumed unless otherwise stated†. The chip rate is 4.096 Mcps and the maximum allowable outage probability o is set at 0.01. The target E_b/I_o depends on the required BER and the adopted performance-enhancing technology. Referring to our computer simulation results [15], we assume γ of 3.34 dB, which corresponds to the voice traffic requiring BER of 10^{-3} when a convolutional code of rate 1/3 and an interleaving length of 10 msec are adopted. Although γ is likely to become smaller in a non-fading environment than in a multipath fading environment, the same value of γ is assumed for numerical examples for a simple and direct comparison.

First, Sect. 5.1 considers a non-fading case for discussing basic performance of a spectrally overlapped system. The bandwidth efficiency is compared between raised cosine spectrum pulse and rectangular chip pulse. And then, Sect. 5.2 proceeds to the evaluation for multipath fading and multiple cell environments.

†The effect of $S_{\max}$ can be found in [11] for a conventional CDMA system

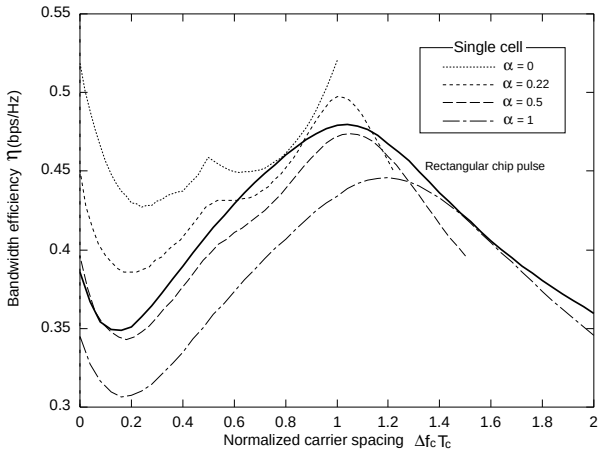

Fig. 3 The bandwidth efficiency of a single cell system ($K = 4$) versus the normalized carrier spacing $\Delta f_c T_c$ for a raised cosine spectrum pulse shaping filter and a rectangular chip pulse.

5.1 Non-fading Environment

5.1.1 Effect of the Roll-off Factor

Figure 3 shows the bandwidth efficiency as a function of the normalized carrier spacing $\Delta f_c T_c$ for various values of α, together with the case of rectangular chip pulse. K is set at 4 for simplicity. The optimum overlapping which maximizes the bandwidth efficiency differs according to the value of α. For example, the optimum overlapping is around $\Delta f_c T_c = 1.2$ for $\alpha = 1$, and it decreases as α decreases, and approaches around 1 for $\alpha = 0.22$. The bandwidth efficiency at optimum overlapping (called here *maximum bandwidth efficiency*) increases as α decreases. For instance, $\alpha = 0$ yields approximately 17 % bandwidth efficiency increase compared to the case $\alpha = 1$. If $\alpha = 0$, overlapping does not give any performance enhancement at all. Coincidentally, the optimum carrier spacing is $1/T_c$ for a rectangular chip pulse as well (i.e., $\Delta f_c T_c = 1$), which is well consistent with the previous results in [8], [9]. However, it should be noted that in the case of rectangular chip pulse, $\Delta f_c T_c = 1$ represents that the optimal overlapping is half the main robe bandwidth as in [8] but it doesn't in the case of raised cosine spectrum pulse because the main robe bandwidth comes to $(1+\alpha)/T_c$ as explained in Sect. 2.3. Table 2 compares the bandwidth efficiency η_0 of a perfectly overlapped system and the maximum bandwidth efficiency for a single cell sys-

Table 2 Comparison of the bandwidth efficiency at $\Delta f_c T_c = 0$, η_0, and the maximum bandwidth efficiency $\eta_{\max}$ (Single cell system: $K = 4$)

	Rectangular chip pulse	Raised cosine filter			
		$\alpha = 0$	$\alpha = 0.22$	$\alpha = 0.5$	$\alpha = 1$
η_0	0.39	0.52	0.45	0.40	0.35
$\eta_{\max}$	0.48	0.52	0.50	0.47	0.45
$\frac{\eta_{\max}}{\eta_0}$	1.23	1	1.11	1.18	1.29

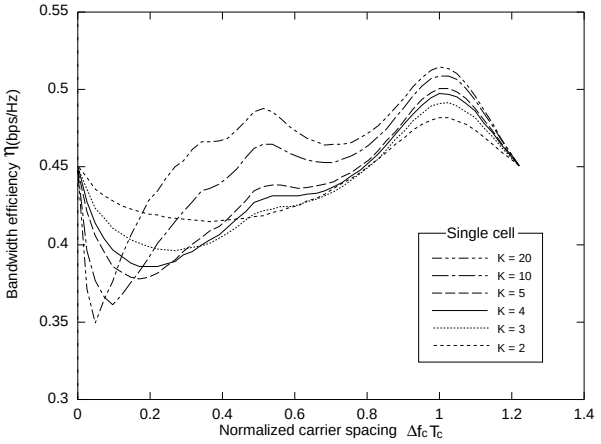

Fig. 4 The effect of the number K of overlapped subsystems for a raised cosine spectrum pulse shape filter with $\alpha = 0.22$.

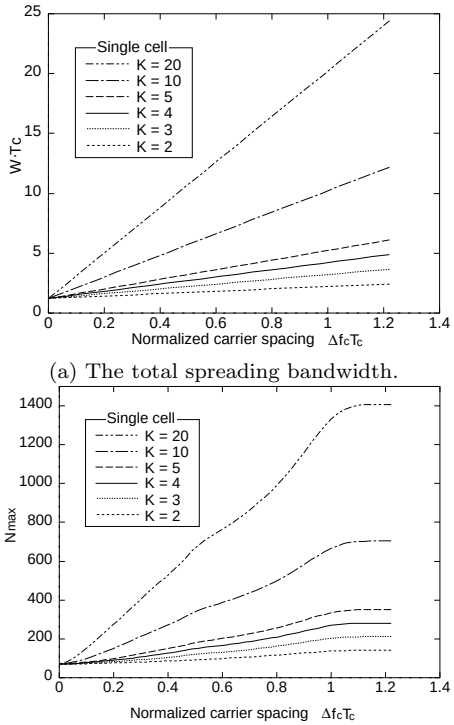

(a) The total spreading bandwidth.

(b) The maximum total number of users.

Fig. 5 The total spreading bandwidth and the maximum total number of users for various values of K ($\alpha = 0.22$).

tem with $K = 4$. η_0 is equivalent to the bandwidth efficiency of a conventional CDMA system. The ratio representing the maximum gain obtainable by overlapping is found to largely depend on the characteristic of pulse shaping.

5.1.2 Effect of the Number of Overlapped Subsystems

The effect of the number K of overlapped subsystems is investigated in Fig. 4, where $\alpha = 0.22$ and equal number of users are assumed to be accommodated in each subsystem. It is interesting to note that the optimum overlapping is independent of K. However, as K increases, the maximum bandwidth efficiency increases and saturates. This will be discussed more in detail later. The trends are different according to K, especially around $\Delta f_c T_c = 0.5$.

To more easily understand this phenomenon, we plot the total spreading bandwidth W and the maximum total number of users $N_{\max}$ in Eq. (15) in Fig. 5. While the total spreading bandwidth linearly increases as $\Delta f_c T_c$ increases, nonlinear increase in $N_{\max}$ can be observed. Since the interference from other subsystems is very small if $\Delta f_c T_c$ is larger than 1 (see Fig. 2), there is only a slight increase in $N_{\max}$ in this range. Similar trend can be observed around $\Delta f_c T_c = 0.5$ due to the interaction between subsystems next but one to each other. This kind of nonlinear increase in $N_{\max}$ yields different trends for different values of K in Fig. 4.

Figure 6 shows the bandwidth efficiency versus the normalized carrier spacing $\Delta f_c T_c$ for various values of K in the case of rectangular chip pulse. Similarly to Fig. 4, there is no change in the optimum overlapping, and the maximum bandwidth efficiency increases and finally saturates as the value of $\Delta f_c T_c$ increases.

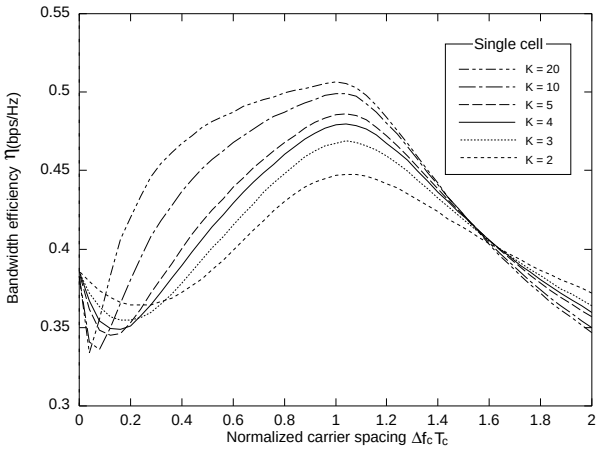

Fig. 6 The effect of the number K of overlapped subsystems for a rectangular chip pulse.

Figure 7 plots the maximum bandwidth efficiency of the single cell system as a function of K for a rectangular chip pulse and a raised cosine spectrum pulse shaping filter with $\alpha = 0.22$. As indicated in Figs. 4 and 6, the maximum bandwidth efficiency increases

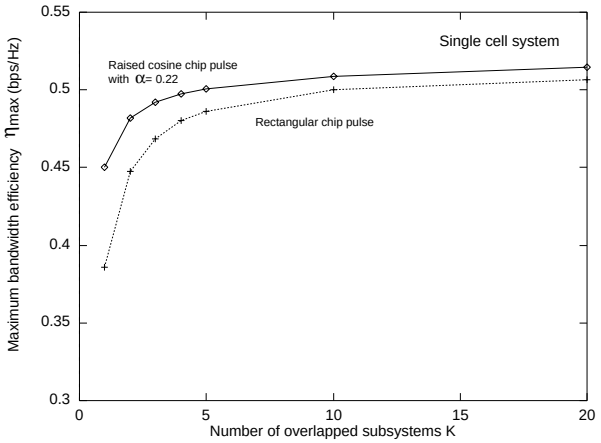

Fig. 7 The effect of the number K of overlapped subsystems on maximum bandwidth efficiency of a single cell system.

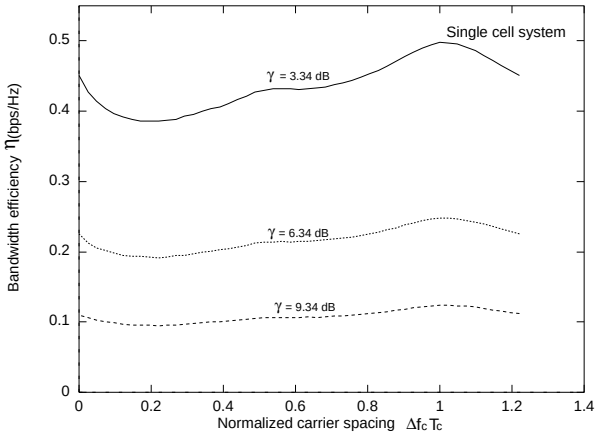

Fig. 8 The bandwidth efficiency of a single cell system ($K = 4$ and $\alpha = 0.22$) versus the normalized carrier spacing $\Delta f_c T_c$ for various values of γ.

and eventually saturates as K increases. When K is changed from 1 to 4, the maximum bandwidth efficiency is increased by 24 % and 10 % for a rectangular chip pulse and a raised cosine spectrum pulse shaping filter with $\alpha = 0.22$, respectively. Comparing the raised cosine spectrum pulse shaping filter with the rectangular chip pulse, the former yields 17 % better performance than the latter when $K = 1$. However, this gain is reduced to 3.6 % and 1.6 % for $K = 4$ and 20, respectively. Therefore, we can see that overlapping helps not only increase the bandwidth efficiency but also mitigate the strict pulse shaping filter problem for large K. Increasing K from 20 to 50 is found to yield only 0.6 % and 1.15 % bandwidth efficiency gain for a raised cosine spectrum pulse shaping filter and a rectangular chip pulse, respectively.

5.1.3 Effect of γ

Figure 8 illustrates the effect of γ on the bandwidth efficiency of a single cell system with $K = 4$ and $\alpha = 0.22$. There is no change in the optimum overlapping for different values of γ. It can be easily understood, from Eq. (7), that the bandwidth efficiency is inversely proportional to γ.

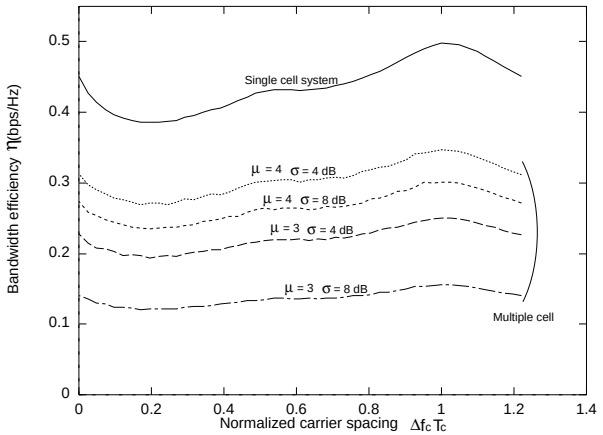

Fig. 9 The bandwidth efficiency for various values of propagation parameters μ and σ ($K = 4$ and $\alpha = 0.22$).

5.1.4 Effect of Propagation Parameters μ and σ

Figure 9 shows the bandwidth efficiency of a multiple cell system for various values of propagation parameters μ and σ. For comparison, the bandwidth efficiency of a single cell system is also plotted. In the multiple cell system, propagation parameters affect the values of $M(\mu, \sigma)$, $A(\mu, \sigma)$, and $B(\mu, \sigma)$ in Eqs. (A· 2) and (A· 3) and therefore, influence the bandwidth efficiency while they do not in the case of single cell system when fast TPC is considered. The optimum overlapping remains at the same value of $\Delta f_c T_c$ irrespective of propagation parameters and it is the same as that of the single cell system. For $\mu = 4$ and $\sigma = 8$ dB, the multiple cell bandwidth efficiency is approximately 60 % of the single cell bandwidth efficiency, which has been already found in [6], [11], [12].

5.2 Multipath Fading Environment

5.2.1 Comparison between Different Power Delay Profile Shapes

Figure 10 shows the bandwidth efficiencies for single and multiple cell systems in non-fading and multipath fading environments when the number R of Rake fingers is equal to L (or $L_{90\%}$) and is set at 4. As discussed in Sect. 4, the bandwidth efficiency of a single cell system is the same for the fading case with a uniform power delay profile and the non-fading case. Although multipath fading increases other cell interference power (see Eqs. (27) and (28)) and accordingly, reduces the bandwidth efficiency, it does not affect the optimum over-

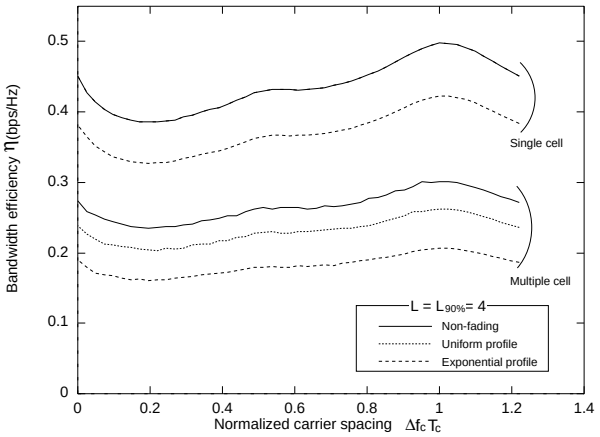

Fig. 10 The bandwidth efficiencies of single and multiple cell systems in non-fading and multipath fading environments ($R = L = L_{90\%}$ =4, $K = 4$, and $\alpha = 0.22$).

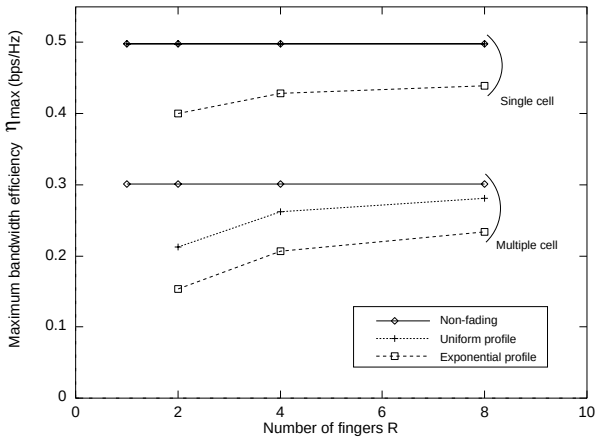

Fig. 11 The maximum bandwidth efficiencies of single and multiple cell systems as a function of the number R of Rake fingers ($R = L = L_{90\%}$, $K = 4$, and $\alpha = 0.22$).

lapping. In a multipath fading environment with an exponential power delay profile, uncaptured multipath components reduce the bandwidth efficiency compared to the case for a uniform power delay profile. The effect of the number of overlapped subsystems with fast TPC is quite different from [8], [9] because fast TPC is assumed to perfectly compensate the variation of the received signal due to multipath fading.

5.2.2 Effect of the Number of Rake Fingers

Figure 11 shows the maximum bandwidth efficiency as a function of the number R of Rake fingers where R is equal to L (or $L_{90\%}$). With ideal fast TPC, since $E[1/X]$ in Eqs. (24), (27), and (28) becomes infinite for L (or $L_{90\%}$) = 1, the bandwidth efficiency becomes zero when L (or $L_{90\%}$) = 1 in the case of multiple cell system (it is also zero when $L_{90\%} = 1$ in the case of single cell system). As more number of resolvable paths exist, the value $E[1/X]$ decreases and therefore, a larger bandwidth efficiency results. In a multiple cell system, increasing R from 2 to 8 yields approximately 32 % gain.

6. Conclusions

In this paper, the reverse link bandwidth efficiency was evaluated for spectrally overlapped CDMA systems with SIR-based fast TPC. The bandwidth efficiency was computed first in a non-fading environment to find the optimum overlapping, i.e., the optimum normalized carrier spacing $\Delta f_c T_c$, for various values of the roll-off factor α of a raised cosine spectrum pulse shaping filter and was compared with the case of rectangular chip pulse. Furthermore, the impact of multipath fading was investigated assuming two different power delay profile shapes for single and multiple cell systems.

It was found that the optimum overlapping does not depend on the power delay profile shape, whether multipath Rayleigh fading exists or not, and whether a single cell or multiple cell system is considered, but the bandwidth efficiency does. And the characteristic of pulse shaping filter largely affects the optimum overlapping and the maximum bandwidth efficiency as well. For example, it is around $\Delta f_c T_c = 1$ for rectangular chip pulse, but it differs according to α for a raised cosine spectrum pulse shaping filter and is around $\Delta f_c T_c = 1$ for $\alpha = 0.22$. Also the number K of subsystems impacts the bandwidth efficiency. When $K = 4$, the raised cosine spectrum pulse shaping filter with $\alpha = 0.22$ yields 3.6 % better performance than the rectangular chip pulse. We could see that overlapping helps to increase the bandwidth efficiency. However, this gain reduces to 1.6 % for $K = 20$. This suggests that the strict pulse shaping filter problem can be avoided for large K.

Multipath fading increases other cell interference power when fast TPC is used and yields smaller bandwidth efficiency than non-fading case. It was found that the bandwidth efficiency is smaller for an exponential power delay profile than for a uniform power delay profile due to uncaptured multipath components when R is equal to L (or $L_{90\%}$) and that the number of paths affects the bandwidth efficiency.

Since the causes of transmission errors are AWGN, ISI, and inter-carrier interference (ICI), the optimal filter combination may exist other than choice of Nyquist filter. This is an interesting future study.

Appendix A: Interference Suppression Factor

From the frequency domain expressions for ξ derived in [10], the interference suppression factor ξ_{ij} from the subsystem i to the subsystem j can be obtained in terms of their composite transfer functions $H_i(f)$ and $H_j(f)$. When the overall filter satisfies Nyquist condition, $H_j(f) = \frac{1}{T_{c,j}}|H_{j,T}(f)|^2 = T_{c,j}|H_{j,R}(f)|^2$, where

the subscripts T and R represent transmitter and receiver, respectively, and $T_{c,j}$ is the chip duration of the subsystem j. Then, ξ_{ij} can be expressed as

$$\xi_{ij} = \frac{\int H_i(f)|H_{j,R}(f)|^2 df}{\int H_i(f)df} = \frac{\int H_i(f)H_j(f)df}{T_{c,j}\int H_i(f)df}. \quad (\text{A}\cdot 1)$$

We assumed asynchronous CDMA systems, where interfering users are asynchronous to the desired user (this is true in the reverse link). Eq. (A·1) can be applied to any kind of chip pulse satisfying Nyquist condition with a known transfer function $H(f)$.

Appendix B: Signal Power and Other Cell Interference Power

Let's consider a system with only a single subsystem (i.e., $K = 1$) for simplicity and ρ denote the spatial density of users given by $\frac{2N}{3\sqrt{3}}$, where N is the number of users of each cell. In a non-fading environment, the mean m_I and the variance σ_I^2 of other cell interference power can be approximated as [11], [12]:

$$m_I \approx M(\mu,\sigma)E[S]N, \quad (\text{A}\cdot 2)$$
$$\sigma_I^2 \approx \left\{A(\mu,\sigma)E[S^2] - B(\mu,\sigma)E^2[S]\right\}N, \quad (\text{A}\cdot 3)$$

where $E[\cdot]$ is an ensemble average operation and $M(\mu,\sigma)$, $A(\mu,\sigma)$, and $B(\mu,\sigma)$ are given by the equations at the top of the next page. r_t is the distance from a user to the t-th BS, and ρ' and $\Phi(x)$ are expressed as:

$$\rho' = \rho/N,$$
$$\Phi(x) = \frac{1}{\sqrt{2\pi}}\int_{-\infty}^{x} e^{-y^2/2}dy.$$

For instance, $M(\mu,\sigma) = 0.659$, $A(\mu,\sigma) = 0.223$, and $B(\mu,\sigma) = 0.04$ when $\mu = 4$ and $\sigma = 8$ dB.

In a multipath fading environment, since *short-term average* interference power from an interfering user of the t-th BS with ideal fast TPC can be expressed as

$$I_t = SE[\frac{1}{X}]\left(\frac{r_t}{r_0}\right)^{\mu} 10^{(\xi_o-\xi_t)/10}, \quad (\text{A}\cdot 4)$$

Eqs. (A·2) and (A·3) can be modified as [20]:

$$m_I \approx E[\frac{1}{X}]M(\mu,\sigma)E[S]N, \quad (\text{A}\cdot 5)$$
$$\sigma_I^2 \approx E^2[\frac{1}{X}]\left\{A(\mu,\sigma)E[S^2] - B(\mu,\sigma)E^2[S]\right\}N, \quad (\text{A}\cdot 6)$$

where X is given in Eq. (19).

References

[1] IEEE Commun. Mag., special issue on Wireless Personal Communications, vol.33, Jan. 1995.
[2] IEEE Pers. Commun., special issue on IMT-2000: Standard Efforts of the ITU, vol.4, Aug. 1997.
[3] IEEE Commun. Mag., special issue on Wideband CDMA, vol.36, Sept. 1999.
[4] L.B. Milstein, D.L. Schiling, R.L. Pickholtz, V. Erceg, M. Kullback, E.G. Kanterakis, D.S. Fishman, W.H. Biederman, and D.C. Salerno, "On the feasibility of a CDMA overlay for personal communications networks," IEEE J. Select. Areas Commun., vol.10, pp.655–668, May 1992.
[5] A. Baier, U.C. Fiebig, W. Granzow, W. Koch, P. Teder, and J. Thielecke, "Design study for a CDMA-based third-generation mobile radio system," IEEE J. Select. Areas Commun., vol.12, pp.733–743, May 1994.
[6] D.K. Kim and F. Adachi, "Capacity estimation for overlaid multiband CDMA systems with SIR-based power control," IEICE Trans. Commun., vol.E83-B, no.7, pp.1454–1464, July 2000.
[7] D.L. Shilling and R.L. Pickholtz, "Improved PCN efficiency through the use of spectral overlay," Proc. ICC, pp.243–244, 1992.
[8] J.H. Han and S.W. Kim, "Optimal spectral overlay of DS/CDMA communication systems," Proc. ICUPC, pp.625–629, 1995.
[9] J.H. Han and S.W. Kim, "Capacity of DS/CDMA communication systems with optimum spectral overlap," IEEE Commun. Letters, vol.2, no.11, pp.298–300, Nov. 1998.
[10] F. Adachi and D.K. Kim, "Interference suppression factor in DS-CDMA systems" Electronics letters, vol.35, pp.2176–2177, Dec. 1999.
[11] D.K. Kim and D.K. Sung, "Capacity estimation for an SIR-based power-controlled CDMA system supporting ON-OFF traffic," IEEE Trans. Veh. Technol., vol.49, no.4, pp.1–8, July 2000.
[12] D.K. Kim and D.K. Sung, "Capacity estimation for a multicode CDMA system with SIR-based power control," IEEE Trans. Veh. Technol., vol.50, no.3, pp.701–710, May 2001.
[13] J.G. Proakis, Digital communications, McGraw-Hill, 3rd Ed., 1995.
[14] Y. Asano, Y. Daido, and J.M. Holtzman, "Performance evaluation for band-limited DS-CDMA communication system," Proc. VTC, pp.464–468, Secaucus, USA, 1993.
[15] A. Shibutani, H. Suda, and F. Adachi, "Multi-stage interleaver for turbo codes in DS-CDMA mobile radio," Proc. APCC/ICCS, pp.391–395, Singapore, Nov. 23-27, 1998.
[16] E. Geraniotis and B. Ghaffari, "Performance of binary and quaternary direct-sequence spread-spectrum multiple-access systems with random signature sequences," IEEE Trans. Commun., vol.39, pp.713–724, May 1991.
[17] F. Adachi, K. Ohno, A. Higashi, T. Dohi, and T. Okumura, "Coherent multicode DS-CDMA mobile radio access," IEICE Trans. Commun., vol.E79-B, pp.1316–1325, Sept. 1996.
[18] C. Kchao and G.L. Stuber, "Analysis of a direct-sequence spread-spectrum cellular radio system," IEEE Trans. Commun., vol.41, pp.1507–1516, Oct. 1993.
[19] F. Adachi, "Transmit power efficiency of fast transmit power controlled DS-CDMA reverse link," IEICE Trans. Fundamen., vol.E80-A, pp.2420–2428, Dec. 1997.
[20] D.K. Kim and F. Adachi, "Theoretical analysis of reverse link capacity for an SIR-based power-controlled cellular CDMA system in a multipath fading environment," IEEE Trans. Veh. Technol., vol.50, no.2, pp.452–464, March 2001.

$$M(\mu,\sigma) = e^{\{\sigma \ln(10)/10\}^2} \iint \left(\frac{r_t}{r_0}\right)^{\mu} \Phi\left(\frac{10\mu}{\sqrt{2\sigma^2}} \log_{10}(r_o/r_t) - \sqrt{2\sigma^2}\frac{\ln(10)}{10}\right) \rho' dA,$$

$$A(\mu,\sigma) = e^{\{\sigma \ln(10)/5\}^2} \iint \left(\frac{r_t}{r_0}\right)^{2\mu} \Phi\left(\frac{10\mu}{\sqrt{2\sigma^2}} \log_{10}(r_o/r_t) - \sqrt{2\sigma^2}\frac{\ln(10)}{5}\right) \rho' dA,$$

$$B(\mu,\sigma) = e^{2\{\sigma \ln(10)/10\}^2} \iint \left(\frac{r_t}{r_0}\right)^{2\mu} \Phi^2\left(\frac{10\mu}{\sqrt{2\sigma^2}} \log_{10}(r_o/r_t) - \sqrt{2\sigma^2}\frac{\ln(10)}{10}\right) \rho' dA.$$

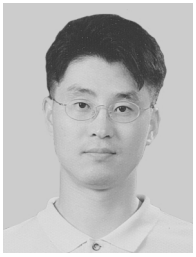

Duk Kyung Kim received the B.S degree in electrical engineering from Yonsei University, Seoul, Korea, in 1992, and the M.S. and Ph.D. degrees from the Korea Advanced Institute of Science and Technology (KAIST), in 1994 and 1999, respectively. From 1999 to 2000, he was a postdoctoral researcher at the Wireless Laboratories, NTT DoCoMo, Japan. From 2000 to 2002, he worked at R&D center, SK Telecom, Korea and involved in the standardization in 3GPP and also in 4G system development. In March 2002, he joined Inha University, Korea. He was interested in Asynchronous Transfer Mode (ATM) network and ATM-based Personal Communication Service (PCS) network. His research interests now include system performance evalution at link/system level, handoff modelling/management, power control, and multi-media provision in CDMA systems and next generation wireless systems

Fumiyuki Adachi received his B.S. and Dr. Eng. degrees in electrical engineering from Tohoku University, Sendai, Japan, in 1973 and 1984, respectively. In April 1973, he joined the Electrical Communications Laboratories of Nippon Telegraph & Telephone Corporation (now NTT) and conducted various types of research related to digital cellular mobile communications. From July 1992 to December 1999, he was with NTT Mobile Communications Network, Inc. (now NTT DoCoMo, Inc.), where he led a research group on wideband/broadband CDMA wireless access for IMT-2000 and beyond. Since January 2000, he has been at Tohoku University, Sendai, Japan, where he is a Professor of Electrical and Communication Engineering at Graduate School of Engineering. His research interests are in CDMA and TDMA wireless access techniques, CDMA spreading code design, Rake receiver, transmit/receive antenna diversity, adaptive antenna array, bandwidth-efficient digital modulation, and channel coding, with particular application to broadband wireless communications systems. From October 1984 to September 1985, he was a United Kingdom SERC Visiting Research Fellow in the Department of Electrical Engineering and Electronics at Liverpool University. From April 1997 to March 2000, he was a visiting Professor at Nara Institute of Science and Technology, Japan. He has published over 170 papers in journals and over 60 papers in international conferences. He has written chapters of three books: Y. Okumura and M. Shinji Eds., "Fundamentals of mobile communications" published in Japanese by IEICE, 1986; M. Shinji, Ed., "Mobile communications" published in Japanese by Maruzen Publishing Co., 1989; and M. Kuwabara ed., "Digital mobile communications" published in Japanese by Kagaku Shinbun-sha, 1992. He was a co-recipient of the IEICE Transactions best paper of the year award 1996 and again 1998. He is a senior member of the IEEE and was a co-recipient of the IEEE Vehicular Technology Transactions best paper of the year award 1980 and again 1990 and also a recipient of Avant Garde award 2000.